



## NRC Publications Archive Archives des publications du CNRC

### **Effect of EGR on heavy-duty diesel engine emissions characterized with laser-induced incandescence**

Neill, W. Stuart; Smallwood, Gregory J.; Snelling, David R.; Sawchuk, Robert A.; Clavel, Dan; Gareau, Daniel; Chippior, Wallace L.

This publication could be one of several versions: author's original, accepted manuscript or the publisher's version. / La version de cette publication peut être l'une des suivantes : la version prépublication de l'auteur, la version acceptée du manuscrit ou la version de l'éditeur.

For the publisher's version, please access the DOI link below. / Pour consulter la version de l'éditeur, utilisez le lien DOI ci-dessous.

#### **Publisher's version / Version de l'éditeur:**

<https://doi.org/10.1115/ICEF2002-532>

*ASME Conference Proceedings. Design, Application, Performance and Emissions of Modern Internal Combustion Engine Systems and Components, ICEF2002-532, pp. 489-497, 2002*

#### **NRC Publications Record / Notice d'Archives des publications de CNRC:**

<https://nrc-publications.canada.ca/eng/view/object/?id=426846fb-88aa-4340-849d-fee8a0cc3444>

<https://publications-cnrc.canada.ca/fra/voir/objet/?id=426846fb-88aa-4340-849d-fee8a0cc3444>

Access and use of this website and the material on it are subject to the Terms and Conditions set forth at

<https://nrc-publications.canada.ca/eng/copyright>

READ THESE TERMS AND CONDITIONS CAREFULLY BEFORE USING THIS WEBSITE.

L'accès à ce site Web et l'utilisation de son contenu sont assujettis aux conditions présentées dans le site

<https://publications-cnrc.canada.ca/fra/droits>

LISEZ CES CONDITIONS ATTENTIVEMENT AVANT D'UTILISER CE SITE WEB.

**Questions?** Contact the NRC Publications Archive team at

PublicationsArchive-ArchivesPublications@nrc-cnrc.gc.ca. If you wish to email the authors directly, please see the first page of the publication for their contact information.

**Vous avez des questions?** Nous pouvons vous aider. Pour communiquer directement avec un auteur, consultez la première page de la revue dans laquelle son article a été publié afin de trouver ses coordonnées. Si vous n'arrivez pas à les repérer, communiquez avec nous à PublicationsArchive-ArchivesPublications@nrc-cnrc.gc.ca.



WR001844

# CISTI ICIST

CT-07782548-0

Document Delivery Service  
in partnership with the **Canadian Agriculture Library**

Service de fourniture de Documents  
en collaboration avec la **Bibliothèque canadienne de l'agriculture**

**THIS IS NOT AN INVOICE / CECI N'EST PAS UNE FACTURE**

MARIA CLANCY  
DGO  
INST FOR CHEM PROCESS & ENVIR TECH  
NATIONAL RESEARCH COUNCIL CANADA  
M-12, ROOM 141, 1200 MONTREAL RD.  
OTTAWA, ON K1A 0R6  
CANADA

**ORDER NUMBER:** CT-07782548-0  
**Account Number:** WR001844  
**Delivery Mode:** XLB  
**Delivery Address:**  
**Submitted:** 2009/03/04 10:02:59  
**Received:** 2009/03/04 10:02:59  
**Printed:** 2009/08/28 07:47:33

<b>Extended</b>	<b>Periodical</b>	<b>Fax - transcribed</b>	<b>CANADA</b>
-----------------	-------------------	--------------------------	---------------

Client Number: MARIA CLANCY MAR 02 2009 # 33  
Author: NEILL W S; SMALLWOOD G J; GULDER O L  
Vol./Issue: ICEF2002-532  
Date: 2002  
Article Title: EFFECT OF EGR ON HEAVY-DUTY DIESEL ENGINE EMISSIONS....  
Series Title: ASME-ICED 2002 FALL TECHNICAL CONFERENCE, NEW ORLEANS, LA, SEP. 2002

**INSTRUCTIONS: \*\*\*\*\*ATTN: MARIA CLANCY\*\*\*\*\***

**Estimated cost for this 9 page document: \$0 document supply fee + \$0 copyright = \$0**

The attached document has been copied under license from Access Copyright/COPIBEC or other rights holders through direct agreements. Further reproduction, electronic storage or electronic transmission, even for internal purposes, is prohibited unless you are independently licensed to do so by the rights holder.

Phone/Téléphone: 1-800-668-1222 (Canada - U.S./E.-U.) (613) 998-8544 (International)  
www.nrc.ca/cisti Fax/Télécopieur: (613) 993-7619 www.nrc.ca/icist  
info.cisti@nrc.ca info.icist@nrc.ca



## EFFECT OF EGR ON HEAVY-DUTY DIESEL ENGINE EMISSIONS CHARACTERIZED WITH LASER-INDUCED INCANDESCENCE

W. Stuart Neill, Gregory J. Smallwood, David R. Snelling, Robert A. Sawchuk,  
Dan Clavel, Daniel Gareau and Wallace L. Chippior

Institute for Chemical Process and Environmental Technology  
National Research Council Canada  
Ottawa, ON Canada

### ABSTRACT

The regulations governing diesel engine particulate matter (PM) and oxides of nitrogen ( $\text{NO}_x$ ) emissions are becoming increasingly stringent. New instrumentation is urgently needed to make accurate and precise measurements of PM emissions from low-emitting engines and emission control systems in a reasonable amount of time.

Laser-induced incandescence (LII) is a technique for making temporally resolved measurements of soot volume fraction. LII offers real-time particulate concentration measurements over several orders of magnitude, and adds desirable information about particulate size and surface area.

In this study, the exhaust gas recirculation (EGR) system of a heavy-duty diesel engine was tuned at eight speed/load conditions using quantitative LII. Soot concentrations measured by LII correlated strongly with measurements taken using the standard gravimetric technique and an AVL smoke meter.

### INTRODUCTION

The diesel engine is an extremely attractive power source for the transportation sector because of its high fuel conversion efficiency. The diesel engine has higher levels of particulate matter (PM) and nitrogen oxides ( $\text{NO}_x$ ) emissions than the spark ignition engine which has led to environmental concerns and increasingly stringent diesel emission standards.

In North America, PM emissions from heavy-duty diesel engines have been reduced by roughly one order of magnitude over the past decade and a further order of magnitude reduction is required by the year 2007. Unfortunately, the manufacturers of engines and emission control systems, as well as regulators, are hampered by the lack of a new standard for measuring low level PM emissions from next-generation powerplants. It is becoming difficult to take accurate PM emission measurements

using the standard gravimetric method in a reasonable amount of time. Moreover, the gravimetric method does not provide the transient PM emissions data required by engine manufacturers to optimize their engines.

Laser-induced incandescence (LII) is a powerful optical diagnostic for studying soot (elemental carbon-based particles emitted from combustion sources) volume fraction in complex combustion flow fields. LII measures the soot volume fraction, active surface area, and primary particle size in real-time under both steady state and transient conditions. LII measurements can be made *in situ* or by continuous sampling, and no dilution or cooling is required. An excellent review of LII theory, experimental approaches and practical applications is available [1].

LII has been successfully applied at the National Research Council Canada (NRC) to measure soot concentrations in various applications covering a range of six orders of magnitude, as shown in Figure 1. The range of applications include laminar diffusion flames [2], carbon black production [3, 4], diesel engine exhaust streams [3, 5, 6], and direct injection spark ignition vehicle exhaust [7]. LII has been shown by Wainner et al. [8] to be sensitive to soot concentrations as low as one part-per-trillion (ppt). The ability to make rapid measurements of extremely low soot concentrations makes LII a preferred method by researchers and a potential soot measurement standard.

Cooled exhaust gas recirculation (EGR) appears to be the method of choice for most North American engine manufacturers to meet the emission standards from heavy-duty diesel engines in 2004. EGR involves reintroducing exhaust gases into the intake charge of the engine. It is known to affect the combustion process in three ways [9]. Firstly, the  $\text{CO}_2$  and

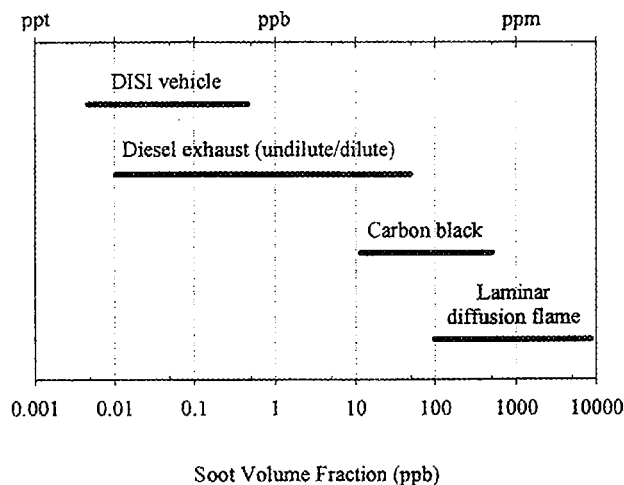


**Figure 1- Range of Soot Volume Fractions Studied by NRC using LII Method (to date)**

H<sub>2</sub>O present in the exhaust decreases the oxygen content in the intake charge. This reduces the NO<sub>x</sub> formation reaction rate during combustion and is known as the dilution effect of EGR. Secondly, the CO<sub>2</sub> and H<sub>2</sub>O from the exhaust dissociate at high temperatures and participate in the combustion process. This is known as the chemical effect of EGR. Thirdly, the specific heats of CO<sub>2</sub> and H<sub>2</sub>O are slightly higher than that of air, which reduces the combustion chamber temperature during the compression stroke. This is known as the thermal effect of EGR. Experiments have shown that the dilution effect is the dominant mechanism that leads to lower NO<sub>x</sub> emissions [9].

Although EGR is an effective technique for reducing NO<sub>x</sub> emissions from diesel engines, it also leads to higher total PM emissions. The increase in total PM emissions is due to higher soot emissions as the EGR rate increases, while the soluble organic fraction (SOF) of PM from the fuel and lubricating oil decreases [10]. Thus, EGR must be applied judiciously at different engine operating modes to reduce NO<sub>x</sub> emissions without excessively increasing PM emissions.

The objective of this study was to measure the effect of EGR on NO<sub>x</sub> and PM emissions from a single-cylinder, heavy-duty, diesel engine. More specifically, the goal was to establish reasonable EGR settings at the eight operating conditions (modes) that comprise the AVL steady-state simulation of the EPA transient test procedure [11] using LII and a standard chemiluminescent analyzer to rapidly measure the soot and NO<sub>x</sub> emissions, respectively.

## EXPERIMENTAL SETUP

### Research Engine

The research engine is a single-cylinder version of the Caterpillar 3400-series, heavy-duty, diesel engine. The engine has a displacement of 2.44 liters, and produces 74.6 kW at

**Table 1- Engine Specifications**

Engine Parameter	Value
Engine Model	Caterpillar 3401
Number of Cylinders	1
Fuel Injection Type	Direct Injection
Number of Valves	4
Combustion Chamber	Mexican Hat
Bore x Stroke	137.2 mm x 165.1 mm
Compression Ratio	16.25:1
Displacement	2.44 liters
Maximum Power Output	74.6 kW @ 2100 rpm

2100 rpm. Further engine details are provided in Table 1. A schematic of the engine setup is provided as Figure 2.

Compressed and temperature-controlled air was supplied to the research engine to simulate the parent engine's turbocharger/intercooler. Surge tanks were fitted at the engine intake and exhaust to minimize pressure pulsations and improve charge pressure control. Intake air mass flow was measured by a turbine flow meter (EG&G Flow Technology, model FT-20C1NA-GEA-1). Intake air and exhaust pressures were controlled using valves to maintain a pumping loop similar to that in a 500-hp version of the 3406E engine.

Diesel fuel was filtered, gravity-fed to a fuel balance (AVL, model 733), and then delivered to the engine's fuel injection pump. A 500 Hz pulse width modulated signal served as the

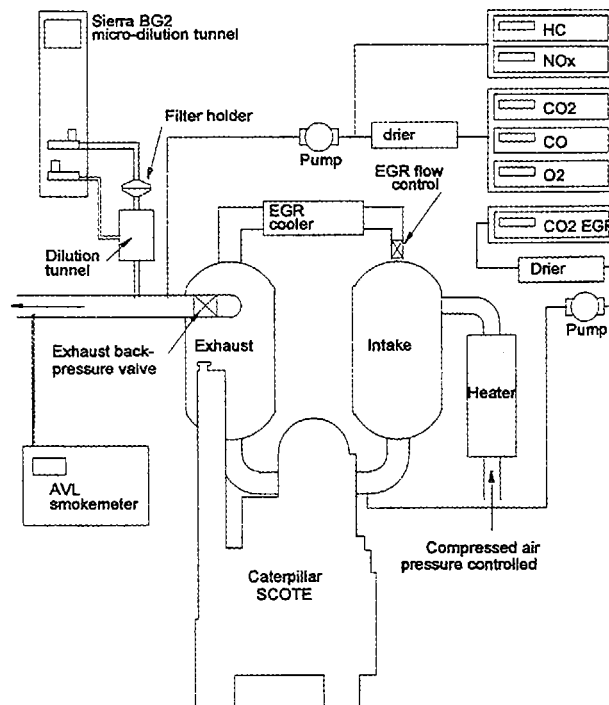


**Figure 2- Schematic of Engine Laboratory Setup**

throttle-input signal to the electronic control module (ECM). The fuel injection timing was adjusted by uploading the desired value into ECM memory using custom software supplied by Caterpillar.

Filtered lubricating oil (Shell Rotella™ T with XLA, 15W-40) was supplied to the engine at a pressure of 400 kPa by an external pump. The lubricating oil was cooled by an integral oil-to-water heat exchanger. An external flow control valve and a 5 kW heater maintained the engine oil at a temperature of 95°C.

Engine coolant temperature was maintained at 85°C using the engine's integral coolant-to-water heat exchanger. The coolant temperature was controlled using a valve that adjusts the water flow to the heat exchanger.

The engine was connected to the dynamometer by a flexible drive coupling (KopFlex Inc., model Holset 3.0 Max-C "CB"). Engine loading was accomplished by an eddy-current dynamometer (Mid-West, model 1014) with a 131 kW rating at 2500 rpm. A load cell (Lebow, model 3169) measured the dynamometer load. Engine speed was measured using a Hall-effect transducer. A DC electric motor was used to start the engine.

### **Exhaust Gas Recirculation System**

A cooled EGR system was realized by directly linking the exhaust and intake surge tanks. EGR is activated by raising the pressure in the exhaust surge tank above the pressure in the intake surge tank. The EGR is driven by the pressure differential between the exhaust and intake surge tanks and is controlled by a flow control valve. The recirculated exhaust gas was cooled using a tube and shell heat exchanger.

Increasing the exhaust back pressure to drive the EGR flow affected engine operation in two ways. Firstly, additional pumping work was required on the exhaust stroke due to the higher back pressure with EGR relative to the normal operating back pressure. A small adjustment to the load set point was made to the modes where the back pressure was increased. Secondly, the increased engine back pressure leads to an increase in the exhaust gas residual between engine cycles, known as internal EGR, which has a much higher temperature than the cooled EGR.

The EGR rates reported in this paper, defined as the volume percentage of the intake air charge that is exhaust gases, are defined as

$$\%EGR = 100 \frac{\%CO_2(\text{intake}) - \%CO_2(\text{ambient})}{\%CO_2(\text{exhaust}) - \%CO_2(\text{ambient})} \quad (1)$$

### **Emissions Instrumentation**

A heated probe was mounted after the exhaust surge tank to sample the gaseous emissions. The exhaust emissions instrumentation (Rosemount, model NGA 2000) consisted of a

chemiluminescent oxides of nitrogen (NO<sub>x</sub>) analyzer, a flame ionization total hydrocarbon (HC) analyzer, a non-dispersive infrared carbon monoxide (CO) analyzer, and a paramagnetic oxygen (O<sub>2</sub>) analyzer. Non-dispersive infrared analyzers were used to measure the carbon dioxide (CO<sub>2</sub>) concentrations in the engine intake and exhaust streams.

Engine soot and particulates were measured using a smoke meter (AVL LIST GmbH, model 415) and a particulate sampling system (Sierra Instruments Inc., model BG-2), respectively. The AVL smoke meter operates by measuring the reflectance of a filter paper, through which a fixed volume of exhaust gas has passed, to determine the degree of blackening. The Sierra system operates by diluting a portion of the exhaust gas with a measured amount of dry, hydrocarbon-free air in a patented dilution chamber and passing the dilute exhaust gas through a pair of 90-mm filter membranes (Pallflex, fiberfilm T60A20). A suitable dilution ratio was selected at each mode to ensure that the sampling temperature at the filters was 52°C or lower. The filters were conditioned before and after sampling in an environmental chamber (Lunaire Ltd., model Tenney BTRS) and were weighed by a microbalance (Sartorius AG, model M5P-000V001).

### **Laser-Induced Incandescence (LII)**

As the LII systems developed at NRC have been described previously [5, 6], only a brief description of the system will be provided. A pulsed Nd:YAG laser, operating with 15 mJ/pulse at 20 Hz and 1064 nm, was used as the excitation source. A half-wave plate (to rotate the plane of polarization) in combination with a thin film polarizer (angle-tuned to transmit horizontally polarized radiation) was used to adjust the laser energy as required. A second half-wave plate was used to return the plane of polarization to vertical. Near top-hat profiles were used for all measurements to deliberately ensure that the soot particles were heated to a uniform temperature throughout the sample volume. A schematic of the LII system may be seen in Figure 3.

The 1064-nm output beam of the Big Sky laser was geometrically filtered by a 1.25 mm wide by 2.35 mm tall slit. Relay imaging of the slit (2:1) was used to generate a 2.5 mm wide by 4.7 mm tall rectangular laser beam at the probe volume with a top hat energy distribution profile. The LII signal from the center of the laser beam was imaged at 2:1 magnification on to a 1 mm diameter aperture, which was direct-coupled to a two-channel demultiplexer detector box. The imaging system was arranged such that the imaging axis was at an angle of 35° from the forward direction of the laser beam.

An optical cell was placed in the line between the dilution tunnel and the PM filter holder. When the laser was pulsed, particulates passing through the center of the cell were heated and the subsequent incandescence was measured. The LII signal was recorded by two photomultipliers, equipped with narrowband interference filters centered at 400 nm and 780 nm,

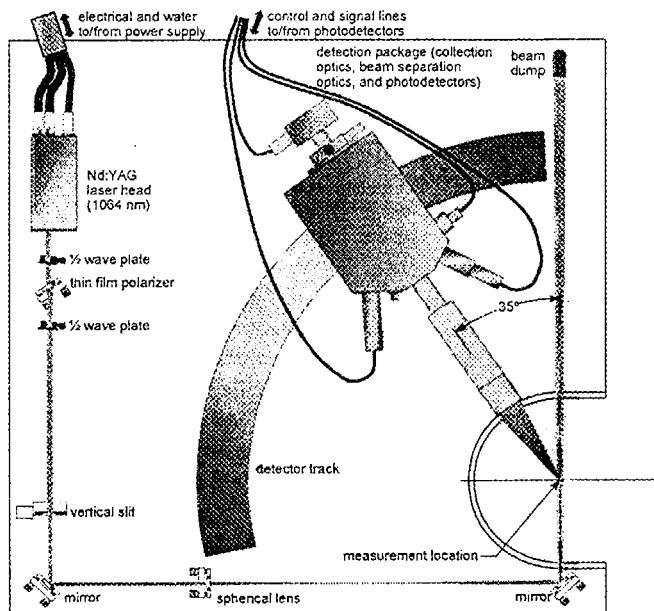


Figure 3- Top-view Schematic of the LII Optical Apparatus

respectively. Transient signals from the photomultipliers were recorded and subsequently transferred to a computer for further analysis. A total of 400 LII signals were collected at each engine operating condition.

### LII Soot Concentration

The methodology to determine the soot concentration is as follows. It is based upon knowledge of the particulate surface temperature, determined by two-wavelength pyrometry. A single point calibration is made in a known source at a known temperature, which results in an absolute sensitivity (in  $W/m^3\text{-ster}$ ). By recording the time-resolved exhaust data at two wavelengths the temperature of the particulate can be determined at any point in time, by solving the following equation

$$\frac{I_{\lambda_1}}{I_{\lambda_2}} = \frac{\lambda_2^6 \left( e^{\frac{hc}{k\lambda_2 T}} - 1 \right) E(m)_{\lambda_1}}{\lambda_1^6 \left( e^{\frac{hc}{k\lambda_1 T}} - 1 \right) E(m)_{\lambda_2}} \quad (2)$$

where  $T$  is the particle surface temperature,  $I_{\lambda}$  is the LII intensity,  $\lambda$  is the detection wavelength,  $E(m)$  is a refractive index dependent function,  $h$  and  $k$  are Planck and Boltzmann constants, respectively, and  $c$  is the velocity of light.  $E(m)$  was assumed to be 0.278 and 0.336 at the detection wavelengths of 400 and 780 nm, respectively, based on experimental data by Krishnan et al. [12].

The radiation,  $P_p$ , from a single primary particle of diameter  $d_p$  and known temperature  $T$  can be determined as

$$P_p(\lambda) = \frac{8\pi^3 c^2 h}{\lambda^6 \left( e^{\frac{hc}{k\lambda T}} - 1 \right)} d_p^3 E(m) \quad (3)$$

The number of primary particles,  $N_p$ , is then determined from the ratio of the experimental intensity to  $P_p$ . The soot volume fraction,  $f_v$ , can then be determined from

$$f_v = \frac{\pi d_p^3}{6} \cdot \frac{N_p}{V} \quad (4)$$

where  $V$  is the sample volume determined by the product of the cross-sectional area of the laser sheet viewed and the sheet thickness. Solving Eq. (3) for  $d_p^3$ , and substituting into Eq. (4), one obtains

$$f_v = \frac{N_p P_p(\lambda) \lambda^6 \left( e^{\frac{hc}{k\lambda T}} - 1 \right)}{48\pi^2 c^2 h E(m) V} \quad (5)$$

In Eq. (5), the product  $N_p P_p(\lambda)$  is the experimentally measured absolute LII intensity. This equation shows that the soot volume fraction may be calculated without knowing the primary particle size. However, the specific surface area and primary particle size,  $d_p$ , can be determined from the decay rate of the soot temperature [6].

The absolute light intensity method [3] developed at NRC for calibrating LII signals applies two-wavelength pyrometry principles to determine the particle temperatures, relating the measured LII signals to the absolute sensitivity of the LII signal collection system as determined with a strip filament lamp. The adoption of this approach provides for continuous self-calibration of the LII technique. This allows lower laser fluences to be used, which results in lower maximum soot temperatures. Thus, issues associated with evaporating a significant portion of the soot are avoided.

### Test Procedure

The effect of EGR on engine  $NO_x$  and PM emissions were investigated at the eight modes that comprise the AVL steady-state simulation of the EPA transient test procedure [11]. The simulation involves measuring the engine emissions at eight speed/load settings, as shown in Figure 4. The engine speed settings varied from a low idle speed (600 rpm or 0%) to the engine's rated speed (1800 rpm or 100%). The emissions data from each mode are weighted as follows:

$$BSE = \frac{\sum (Emission Rate)_i \times WF_i}{\sum (Brake Power)_i \times WF_i} \quad (6)$$

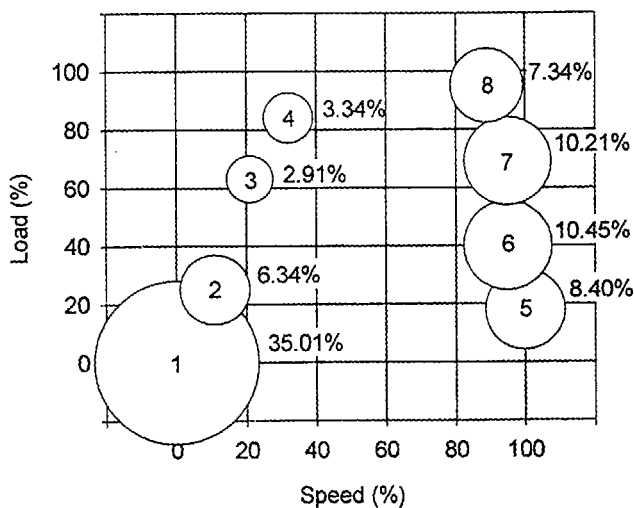


**Figure 4- AVL Eight-Mode Steady-State Simulation**

The weighting scheme, shown in Figure 4, was designed to produce composite brake specific emissions that accurately predict the gaseous emissions obtained using the EPA transient test procedure. (The emissions from the 16.00% motoring portion of EPA transient test procedure are neglected). The steady-state simulation offers information on pollutant formation at different engine operating modes, but does not measure transient engine behaviour. As such, the composite PM emissions can only be expected to show the correct trends because engine transients play a large role in PM production.

In this experiment, the AVL eight-mode steady-state test was performed and repeated once with the engine in its baseline configuration (no EGR). LII soot concentrations were correlated with gravimetric PM emissions. Then, the effect of EGR on emissions was studied at each engine mode by measuring the  $\text{NO}_x$  and PM emissions for several EGR settings. Due to time limitations, the soot mass concentrations were measured using the LII method and an AVL smoke meter. Finally, the AVL eight-mode test was performed and repeated once at the conclusion of the experiment, using the final EGR rates selected, to quantify the trade-off between composite  $\text{NO}_x$  and PM emissions achieved through the application of cooled EGR.

## RESULTS AND DISCUSSION

### LII - Gravimetric Method Correlation (no EGR)

A comparison between LII soot mass concentration and standard gravimetric PM mass concentration at the eight modes is shown in Figure 5. The soot mass concentrations measured by the LII method were lower than the PM mass concentrations measured by the gravimetric method at all eight modes. This result was anticipated because the gravimetric method measures the sum of the carbonaceous (soot) fraction, the adsorbed

hydrocarbons from the fuel and lubricating oil (SOF) and the sulphate fraction, whereas the LII method measures only the soot mass concentration. In this particular experiment, the fuel contribution to sulphate emissions was extremely low because the test fuel had a sulphur content of 3 ppm by mass.

The largest discrepancy between the LII and gravimetric methods occurred at mode 1. This result is not surprising because the PM emissions from diesel engines are known to contain a high percentage of soluble organic components at the low idle condition.

PM filter samples from each of the eight modes were subjected to a solvent extraction procedure to remove the SOF. The extraction was accomplished using an accelerated solvent extraction (ASE) system (Dionex Corp., model 200). The extractions were done for 15 minutes at 1000 C and 2000 psi using dichloromethane as the solvent. Blank filters were also subjected to the same procedure to estimate the filter material lost during the extraction procedure. The PM filters were weighed before and after the extraction procedure using a microbalance and a correction was applied to account for the blank filter weight loss. This resulted in an estimate of the SOF mass.

Figure 6 compares the LII soot concentration to the soot fraction of the gravimetric PM mass concentration for the same two tests. As expected, there is a much better correlation between the two methods after the estimated SOF contribution to the total PM mass concentration is removed. However, the

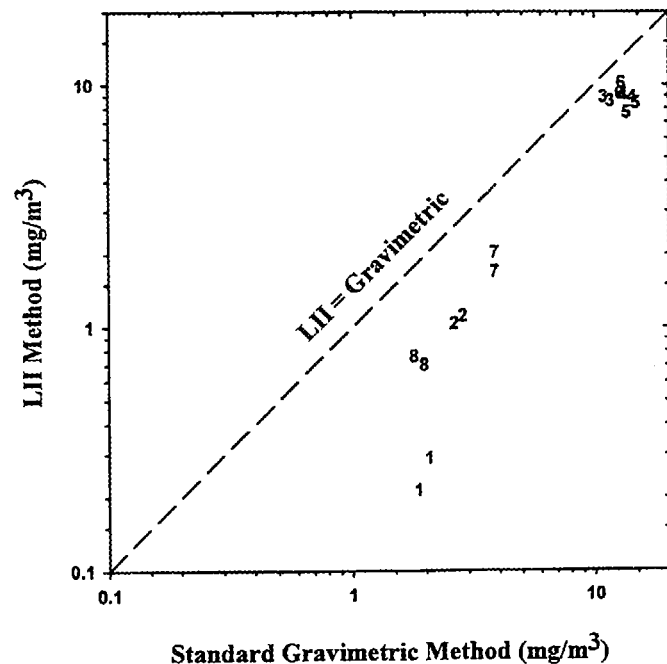


**Figure 5- Comparison between LII Soot Concentration and Gravimetric PM Concentration**

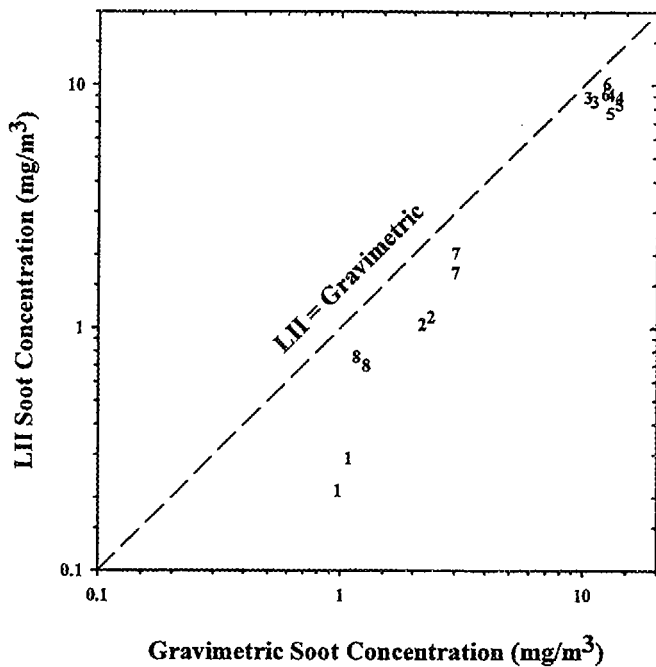


**Figure 6- Comparison between LII Soot Concentration and Gravimetric Soot Concentration**

soot concentrations measured by LII seem to be lower than those measured by the gravimetric method by a relatively constant factor, except at mode 1. The larger discrepancy between methods at mode 1 may be related to the poor accuracy in estimating the soot fraction by the gravimetric method due to the small mass of PM collected at this mode.

**Effect of EGR % on NO<sub>x</sub>-Soot Trade-off**

The effect of EGR on the NO<sub>x</sub> - soot trade-off was investigated at the eight steady-state test modes. In this section, the NO<sub>x</sub> and soot emissions data are plotted as a function of the EGR rate at low speed, low load (mode 2) and high speed, high load (mode 7) operating conditions. The complete data set is provided in Tables A-1 and A-2. Finally, the NO<sub>x</sub> - soot trade-off is shown for all eight modes following the discussion about modes 2 and 7.

**Mode 2**

Mode 2 is a low speed (732 rpm), low load (55 N-m), engine operating condition. Figure 7 shows that the NO<sub>x</sub> emissions from the engine decrease linearly from 540 to 235 ppm as the EGR rate increases from 0 to 30%. Conversely, the LII soot concentrations increased from 0.3 to 1.0 ppb over the same range of EGR rates. Fairly high EGR rates (25% or more) may be utilized at mode 2 because the exhaust soot concentrations are only 0.3 ppb in the absence of EGR and only

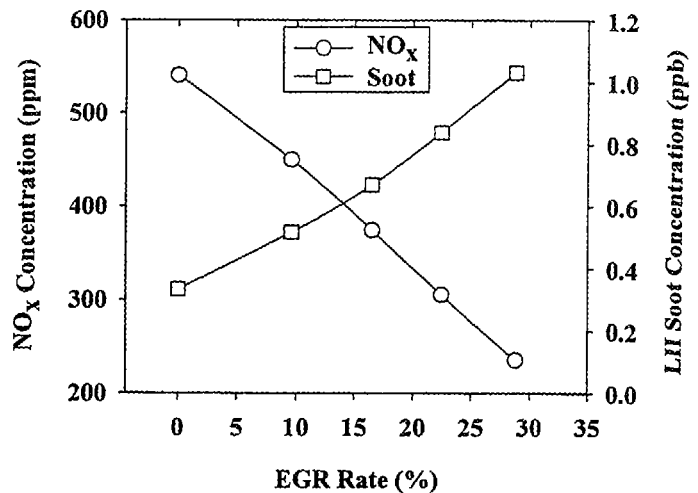


**Figure 7- NO<sub>x</sub> and Soot Concentrations vs. EGR Rate at Mode 2**

increase linearly with EGR up to 30% EGR by volume as shown in the figure.

**Mode 7**

Mode 7 is a high speed (1740 rpm), high load (245 N-m) engine operating condition. Figure 8 shows that the NO<sub>x</sub> concentration decreases linearly from 505 to 235 ppm as the EGR rate is increased from 0 to 15%. In contrast, the soot concentration measured by LII seems to increase linearly for EGR rates up to about 5 or 6%, but then begins to increase exponentially for higher EGR rates. The exponential increase in soot emissions at mode 7 for higher EGR rates is likely due to the reduced oxygen concentration in the intake air charge as the EGR rate is increased. Since the equivalence ratio is much higher at mode 7 than at mode 2, the engine is less tolerant to higher EGR rates (and less excess oxygen). At 15% EGR, the

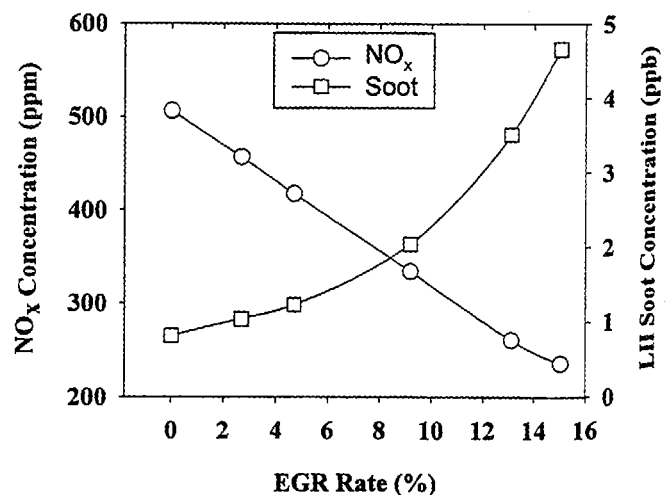


**Figure 8- NO<sub>x</sub> and Soot Concentrations vs. EGR Rate at Mode 7**

exhaust soot concentration is approximately one order of magnitude higher at mode 7 than at mode 2.

### All Modes

Figure 9 shows the  $\text{NO}_x$  - soot trade-off at the eight modes of the AVL steady-state simulation. The graph clearly indicates that EGR reduces the  $\text{NO}_x$  concentration in the diesel engine exhaust at all modes, but that the resultant increase in exhaust soot concentration depends strongly on the engine mode.

Modes 1 and 2 (low speed, low load) are characterized by very low equivalence ratios, low exhaust  $\text{NO}_x$  concentrations, and exhaust soot concentrations below 1 ppb. High EGR rates may be applied at these conditions to reduce the exhaust  $\text{NO}_x$  concentration without dramatically increasing the soot concentration.

Modes 3 and 4 (low speed, high load) are operating conditions with relatively high equivalence ratios, high exhaust  $\text{NO}_x$  concentration and correspondingly high exhaust soot concentrations. Figure 9 shows that the soot concentration increases significantly as the EGR rate increases at these modes. Thus, EGR rates must be limited at these two operating conditions to achieve an acceptable  $\text{NO}_x$  - soot emission trade-off.

At modes 5 and 6 (high speed, low load), the equivalence ratios and exhaust  $\text{NO}_x$  concentrations are fairly low. However, exhaust soot concentrations are higher at modes 5 and 6 than at modes 1 and 2 due to the reduced time available for soot oxidation to occur. As a result, engine soot concentrations start to increase exponentially at lower levels of EGR at modes 5 and

6 than occurs at modes 1 and 2, as shown in the figure.

Modes 7 and 8 (high speed, high load) are characterized by medium equivalence ratios because the turbocharger (simulated in this case) boost pressure is very high. The additional oxygen available for soot oxidation leads to reduced exhaust soot concentrations, relative to modes 3 and 4, and allows somewhat more EGR to be applied.

### Correlation between LII and AVL Smoke Meter

Soot concentrations measured by LII and an AVL smoke meter are compared in Figure 10 for all of the engine modes and EGR settings reported in Table A-1. This graph shows that there was excellent correlation between the two measurement techniques over 2.5 orders of magnitude variation in soot concentration. The coefficient of determination ( $r^2$ ) was 0.95, which provides strong evidence of a linear relationship between the two soot measurement techniques.

Comparing the solid regression line in Figure 10 to the dashed line representing perfect agreement between the two methods, it appears that the soot concentrations measured by LII are 33% lower than those measured by the AVL smoke meter over the entire measurement range. Since LII also measured lower soot concentrations than the gravimetric method, it is likely that part of the difference may be due to the uncertainty in  $E(m)$  with the LII method. Two advantages of the LII method are its sensitivity to very low soot concentrations and its excellent temporal resolution. The AVL smoke meter and the gravimetric technique, on the other hand, require longer sample times as the exhaust soot concentration decreases.

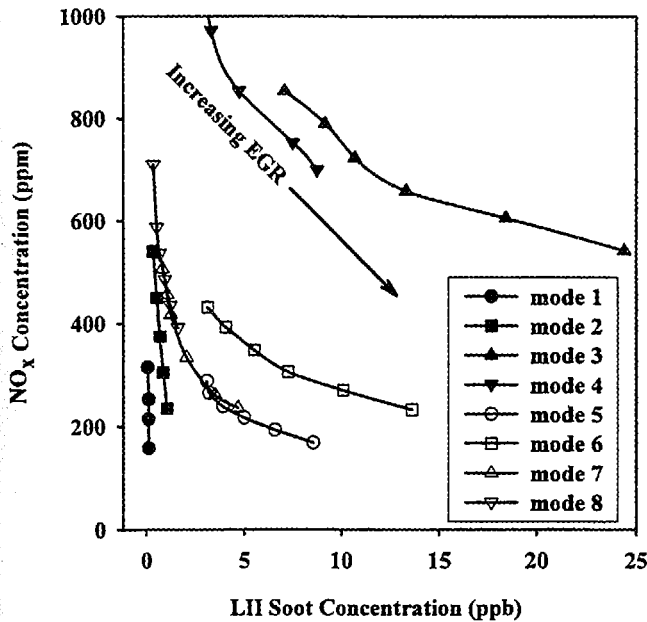


Figure 9-  $\text{NO}_x$  and Soot Concentrations vs. EGR Rate at all 8 Modes

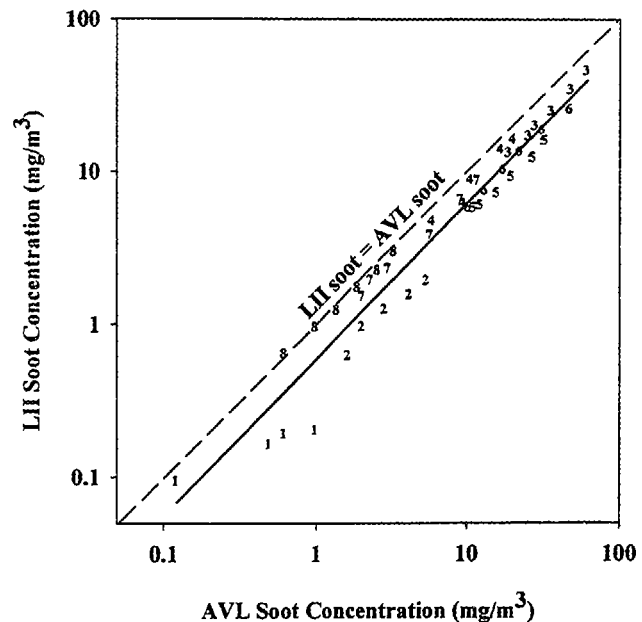


Figure 10- LII Soot Concentration vs. AVL Smoke Meter Soot Concentration

Two potential sources of error have been identified in the soot concentrations measured by the LII method. Firstly, the calculated LII particle intensity is sensitive to errors in the soot surface temperature. The total black body radiation scales as  $T^4$ , so that a maximum 4% error in temperature results in a 16% error in intensity. Secondly, the particulate volume fraction is inversely proportional to  $E(m)$ , and thus a 30% decrease in  $E(m)$  would result in a 30% increase in the measured soot concentration. Recent results have indicated that the value of  $E(m)$  is lower than previously thought and experiments will be performed to obtain a more accurate value in the near future.

### Composite Emissions (EGR vs. Baseline)

The engine  $\text{NO}_x$  and PM emissions were compared with and without EGR at the eight modes of the steady-state simulation. The composite emissions were then calculated for the two cases using Eq. 5 and the weighting factors provided in Figure 4. The effect of EGR was to reduce the composite engine  $\text{NO}_x$  emissions by almost one-half (-42%), however, the PM emissions almost doubled (+90%). The composite  $\text{NO}_x$  and PM emissions results, with and without EGR, are provided in Table 2.

Table 2- Effect of EGR on Composite Emissions

	Baseline Engine	Engine with EGR	% Difference
$\text{NO}_x$ (g/hp-hr)	4.25	2.46	-42
PM (g/hp-hr)	0.040	0.076	90

### CONCLUSIONS

The effect of exhaust gas recirculation on the  $\text{NO}_x$  and particulate matter (PM) emissions from a heavy-duty, single cylinder, diesel engine was investigated at the eight modes of the AVL steady-state simulation of the EPA Transient Test Procedure. A laser-induced incandescence (LII) method developed at NRC and a standard chemiluminescent analyzer measured the soot and  $\text{NO}_x$  emissions, respectively. The main findings of this study are:

1. The LII method provided rapid, precise soot emission measurements from a heavy-duty diesel engine at a variety of speed/load conditions and EGR settings. The final EGR rates selected at the eight modes, based on the previously collected  $\text{NO}_x$  - soot trade-off data, produced composite  $\text{NO}_x$  emissions that were 42% lower than those from the engine with no EGR, but there was a 90% increase in PM emissions.
2. LII exhaust soot concentrations correlated strongly ( $r^2 = 0.95$ ) with soot concentrations measured by an AVL smoke meter over 2.5 orders of magnitude variation in soot concentration.
3. LII exhaust soot concentrations also correlated well with gravimetric residual carbon concentrations after extracting

the SOF from the PM filter samples. The agreement was not as good at mode 1, likely due to uncertainties in determining the SOF at this mode.

### ACKNOWLEDGMENTS

This work was supported by the National Research Council Canada, the Government of Canada's PERD program (Advanced Transportation Task, AFTER POL), Shell Canada Ltd., Syncrude Canada Ltd., Suncor Energy Inc., Imperial Oil Ltd., and the National Centre for Upgrading Technology.

### REFERENCES

- [1] Kohse-Höinghaus, K. and Jeffries, J.B., *Applied Combustion Diagnostics*, Taylor and Francis, New York, 2002.
- [2] Snelling, D. R., Thomson, K. A., Smallwood, G. J. and Gülder, Ö. L., "Two-Dimensional Imaging of Soot Volume Fraction in Laminar Diffusion Flames," *Applied Optics*, 38, pp.2478-2485, 1999.
- [3] Snelling, D. R., Smallwood, G. J. Gülder, Ö. L., Liu, F., and Bachalo, W. D., "A Calibration-Independent Technique of Measuring Soot by Laser-Induced Incandescence Using Absolute Light Intensity," The Second Joint Meeting of the US Sections of the Combustion Institute, Oakland, California, March 25-28, 2001.
- [4] Snelling, D. R., Smallwood, G. J., Gülder, Ö. L., Bachalo, W. D., and Sankar, S., "Soot Volume Fraction Characterization Using the Laser-Induced Incandescence Detection Method," *Proceedings of the 10th International Symposium on Applications of Laser Techniques to Fluid Mechanics*, Lisbon, July, 2000.
- [5] Snelling, D. R., Smallwood, G. J., Sawchuk, R. A., Neill, W. S., Gareau, D., Chippior, W. L., Liu, F., Gülder, Ö. L., and Bachalo, W. D., "Particulate Matter Measurements in a Diesel Engine Exhaust by Laser-Induced Incandescence and the Standard Gravimetric Procedure," *SAE Paper No. 1999-01-3653*, 1999.
- [6] Snelling, D. R., Smallwood, G. J., Sawchuk, R. A., Neill, W. S., Gareau, D., Clavel, D., Chippior, W. L., Liu, F., Gülder, Ö. L. and Bachalo, W. D., "In-Situ Real-Time Characterization of Particulate Emissions from a Diesel Engine Exhaust by Laser-Induced Incandescence," *SAE Paper No. 2000-01-1994*, 2000.
- [7] Smallwood, G.J., Snelling, D.R., Gülder, Ö. L., Clavel, D., Gareau, D., Sawchuk, R.A. and Graham, L., "Transient Particulate Matter Measurements from the Exhaust of a Direct Injection Spark Ignition Automobile", *SAE Paper No. 2001-01-3581*, 2001.
- [8] Wainner, R.T., Seitzman, J.M. and Martin, S.R., "Soot Measurements in a Simulated Engine Exhaust using Laser-Induced Incandescence", *ALAA Journal*, Vol. 37, No. 6, pp. 738-743, 1999.
- [9] Ladommatos, N., Abdelhalim, S. and Zhao, H., "The effects of exhaust gas recirculation on diesel combustion and

emissions", *Int'l Journal of Engine Research*, Vol. 1, No. 1, pp. 107-126, 2000.

[10] Kreso, A.M., Johnson, J.H., Gratz, L.D., Bagley, S.T., and Leddy, D.G., "A Study of the Effects of Exhaust Gas Recirculation on Heavy-Duty Diesel Engine Emissions", SAE Paper No. 981422, 1998.

[11] Cartellieri, W., Krieger, W. and Schweinzer, F., "Strategies to Meet Worldwide Heavy-Duty Diesel Emission Standards", *Proc. Instn. Mech. Engrs.*, Vol. 206, pp. 161-171, 1992.

[12] Krishnan, S.S., Lin, K.C., and Faeth, G.M., "Extinction and Scattering Properties of Soot Emitted from Buoyant Turbulent Diffusion Flames", *Journal of Heat Transfer*, Vol. 123, pp. 331-339, 2001.

**Table A-1- NO<sub>x</sub> – Emission Trade-off vs. EGR Rate**

AVL mode	EGR Rate (%)	NOx Concentration (ppm)	Soot Concentration (ppb)
1	0.0	315	0.15
1	30.4	252	0.1
1	40.0	214	0.1
1	49.9	158	0.1
2	0.0	540	0.3
2	9.6	450	0.5
2	16.5	375	0.7
2	22.4	306	0.8
2	28.8	235	1.0
3	0.0	991	n/a
3	2.2	853	7.1
3	3.3	789	9.2
3	4.4	722	10.7
3	5.5	658	13.3
3	6.5	605	18.4
3	7.5	542	24.4
4	0.0	1194	25.3
4	3.3	972	3.3
4	4.9	853	4.7
4	6.1	752	7.5
4	7.0	699	8.8

**Table A-2- NO<sub>x</sub> – Emission Trade-off vs. EGR Rate**

AVL mode	EGR Rate (%)	NOx Concentration (ppm)	Soot Concentration (ppb)
5	0.0	287	3.1
5	3.7	264	3.2
5	7.9	238	3.9
5	11.7	217	6.0
5	15.6	193	6.6
5	19.8	168	8.5
6	0	432	3.1
6	2.9	393	4.0
6	6.0	348	5.5
6	9.1	306	7.3
6	12.0	270	10.1
6	15.2	232	13.6
7	0.0	506	0.8
7	2.7	457	1.0
7	4.7	417	1.2
7	9.2	334	2.0
7	13.1	261	3.5
7	15.0	236	4.7
8	0.0	710	0.3
8	3.9	588	0.5
8	5.4	536	0.6
8	7.0	486	0.9
8	8.6	435	1.2
8	10.0	392	1.6